Atmos. Chem. Phys. Discuss., https://doi.org/10.5194/acp-2018-762
Manuscript under review for journal Atmos. Chem. Phys.
Discussion started: 3 September 2018

Atmospheric Chemistry and Physics
Discussions

The vertical variability of ammonia in urban Beijing, China

Yangyang Zhang[1], Aohan Tang[1,*], Dandan Wang[1], Qingqing Wang[2], Katie Benedict[3], Lin Zhang[4], Duanyang Liu[5], Yi Li[6], Jeffrey L. Collett Jr.[3], Yele Sun[2,*], Xuejun Liu[1,*]

[1]Beijing Key Laboratory of Farmland Soil Pollution Prevention and Remediation, College of Resources and Environmental Sciences, China Agricultural University, Beijing 100193, China

[2]State Key Laboratory of Atmospheric Boundary Layer Physics and Atmospheric Chemistry, Institute of Atmospheric Physics, Chinese Academy of Sciences, Beijing 100029, China

[3]Department of Atmospheric Science, Colorado State University, Fort Collins, CO80523, USA

[4]Laboratory for Climate and Ocean–Atmosphere Studies, Department of Atmospheric and Oceanic Sciences, School of Physics, Peking University, Beijing 100871, China

[5]Jiangsu Meteorological Observatory, Nanjing 210008, China

[6]Sunset CES Inc., Beaverton, OR97008, USA

[*]*Corresponding authors* (aohantang@cau.edu.cn, sunyele@mail.iap.ac.cn, liu310@cau.edu.cn)

Abstract. Weekly vertical profiles of ammonia (NH_3) were measured at 16 heights on the Beijing 325 m meteorological tower for one year from March 2016 to March 2017. Measured average NH_3 concentrations at all heights exceeded 5 μg m^{-3} with an overall average (±1σ) tower concentration of 13.3±4.8 μg m^{-3}. The highest NH_3 concentrations along the vertical profiles mostly occurred at 32-63 m, decreasing both towards the surface and at higher altitudes. Significant decreases in NH_3 concentrations were only found at the top two heights (280 and 320 m). These results suggest an ammonia rich atmosphere during all seasons in urban Beijing, from the ground to at least 320 m. Highest concentrations were observed in summer, associated with high temperature. The average NH_3 concentration across the profile from high to low was observed in summer (18.2 μg m^{-3}), spring (13.4 μg m^{-3}), autumn (12.1 μg m^{-3}), and winter (8.3 μg m^{-3}). Significant vertical variation of NH_3 concentration was only found in summer. Transport analyses suggest that air masses arriving from intensive agricultural regions to the south contribute high NH_3 concentrations in Beijing. Local sources such as traffic emissions also appear to be important contributors to atmospheric NH_3 in this urban environment.

1. Introduction

Ammonia (NH_3) has long been recognized as an important form of reactive nitrogen (Nr) in atmospheric environment, playing a key role in biogeochemical cycles from atmospheric chemical processes to deposition and subsequent environmental impacts (e.g. air pollution, reduced biodiversity, acidification, and eutrophication) (Fowler et al., 2009; Sutton et al., 2008). NH_3 reacts with nitric and sulfuric acids in air, forming secondary inorganic aerosols (e.g., NH_4NO_3, $(NH_4)_2SO_4$) with long atmospheric lifetimes that can transport these species far from sources and contribute 40-57% of fine particle matter in megacities (Fowler et al., 2009; Huang et al., 2014; Yang et al., 2011). Therefore, NH_3 has received increasing attention in air pollution research (Wang et al., 2015). In addition to agriculture, which is considered the largest NH_3 source globally, emissions from biomass burning, industries, vehicles, and other sources (Galloway et al., 2003; Sutton et al., 2008; Erisman et al., 2008; Sun et al., 2016; Sun et al., 2017) can also be significant.

In China annual NH_3 emissions were approximately 2-3 times higher than European and US emissions over the period 1990 to 2005, and estimated at 15.6 ±0.9 Tg N yr^{-1} in 2015 (Reis et al., 2009; Kang et al., 2016; Zhao and Wang, 1994; Klimont, 2001; EMEP; USEPA, 2009; Zhang et al., 2017). Such high emissions, together with the important role NH_3 plays in degrading air quality, make NH_3 a key target to curb serious air pollution in Chinese urban areas (Fu et al., 2017; Chang et al., 2016; Ye et al., 2011; Wang et al., 2011). Some studies have indicated that reducing NH_3 concentrations could be an effective method for alleviating secondary inorganic $PM_{2.5}$ pollution in China (Gu et al., 2014; Wang et al., 2015; Wu et al., 2016; Xu et al., 2017). NH_3 has received less attention from the government, however, than SO_2 and NO_x, which have been controlled since 2005 and been effectively reduced during the 12th Five-Year Plan period (2011-2015) (Fu et al., 2017). Currently there are strong arguments about the role of regional transport in contributing to haze pollution in China (Guo et al., 2014; Li et al., 2015), especially for severe haze episodes occurring during stagnant meteorological conditions with a shallow boundary layer (Sun et al., 2014; Zheng et al., 2015; Quan et al., 2013). Vertical characterization of air pollutant concentration profiles may be helpful for elucidating factors contributing to the formation and transport of regional haze events (Quan et al., 2013; Tang et al., 2015; Wiegner et al., 2006). Many studies have been conducted to improve understanding of temporal and spatial concentration dynamics of atmospheric NH_3 and how they relate to underlying factors (e.g. emission intensity, meteorological conditions, etc.) and air quality (Yamamoto et al., 1988; Yamamoto et al., 1995; Bari et al., 2003; Vogt et al., 2005; Lee et al., 1999). However, such studies in China have generally focused on the spatial distribution of NH_3 near the ground (Ianniello et al., 2010; Wu et al., 2009; Meng et al., 2011; Xu et al., 2015).

As a trace gas with both point and non-point sources, as well as a tendency to deposit rapidly to surfaces, NH_3 mixing ratios may vary significantly as a function of height. In urban locations, like Beijing, where NH_3 is a key contributor to fine particle formation, local (e.g., traffic) sources emit at the surface and are then mixed through the boundary layer, while NH_3 transported from agricultural sources outside the city are presumably already mixed through the boundary layer. The influence of these behaviors may be reflected in vertical NH_3 concentration gradients measured within the city. For example, dominant local surface traffic emissions might give rise to a profile that peaks near the surface, while ammonia transported into the urban area may be uniformly mixed in the vertical or even decline near the surface due to loss by dry deposition. Of course these patterns are expected to be further affected by sinks, including surface deposition as well as fine particle formation of ammonium salts. NH_3 vertical distribution measurements are also useful for advancing satellite retrievals, which offer great potential for understanding the global distribution of gaseous NH_3 (Shephard and Cady-Pereira, 2015; Sun et al., 2015; Van Damme et al., 2015).

To our knowledge there are few studies reporting long-term observations of vertical distributions of NH_3 in the lowest few hundred meters of the atmosphere, including measurements at the BAO tower in the USA (Li et al., 2017; Tevlin et al., 2017) and CESAR in The Netherlands (Dammers et al., 2017). Li et al. (2017) analyzed vertical NH_3 concentration profiles at the BAO tower in Colorado, USA, reporting the minimum concentration at the top of the tower, slowly increasing towards a peak concentration at ~10 m before a large reduction in concentration at 1 m. The site was influenced by transport of high ammonia concentrations from large animal feeding operations to the northeast. Through higher time resolution measurements at the BAO tower, Tevlin et al. (2017) pointed out that the surface can act as an occasional NH_3 sink as well as a source. The CESAR study in the Netherlands showed that vertical profile differences were mainly due to local and regional transport influence (Li et al., 2017). Because the BAO and CESAR tower sites are both located in a suburban area with low aerosol mass loadings, observed vertical profiles of aerosol and gas species (Öztürk et al., 2013;

VandenBoer et al., 2013; Riedel et al., 2013) could be substantially different from those in megacities in China. Zhou et al. (2017) measured vertical concentration profiles of NH_3 and seven other air pollutants at ten heights (8, 15, 47, 80, 120, 160, 200, 240, 280 and 320 m) in urban Beijing, finding NH_3 concentrations peaked at 160 m. However, the observation period was too short (two weeks) to investigate seasonal variations and may not adequately represent typical conditions. Until now, long-term monitoring of vertical NH_3 concentration profiles has not been carried out in China.

Here, we report a one-year field campaign on the Beijing 325 m meteorological tower to investigate vertical NH_3 concentration profiles and consider how temporal variations may relate to urban emission sources, meteorological factors and air transport from more distant sources. Study findings are relevant for our understanding of precursor ammonia distributions and the role of ammonia in the formation of severe aerosol pollution in China, and further provide benchmarks to assist in meeting air quality goals and policy needs in future.

2. Materials and methods

2.1 Site Description

The sampling site is located at the State Key Laboratory of Atmospheric Boundary Layer Physics and Atmospheric Chemistry (LAPC), Institute of Atmospheric Physics (IAP), Chinese Academy of Sciences (CAS) in urban Beijing (39°58′ N, 116°22′E) (Fig. 1). The site is approximately 0.8 km north of the third Ring Road and 1.3 km south of the fourth Ring Road, major transport arteries encircling Beijing, each with average traffic volumes of approximately 10 million vehicles day^{-1}, representing a typical urban site surrounded mainly by residential areas.

2.2 NH_3 measurement

From March 16, 2016 to March 16, 2017, weekly atmospheric NH_3 samples were collected at 16 heights on the 325 m meteorological tower using ALPHA passive samplers (adapted low-cost high absorption, Centre for Ecology and Hydrology, Edinburgh, UK). NH_3 was sampled at 2, 8, 15, 32, 47, 63, 80, 102, 120, 140, 160, 180, 200, 240, 280, and 320 m above ground level. At each height, three ALPHA samplers were deployed under a PVC shelter to protect the samplers from rain and direct sunlight (shown in Fig. 1). Collected NH_3 samplers were extracted with 10 mL high-purity water (18.2

MΩ-cm) and analyzed using a continuous-flow analyzer (Seal AA3, Germany). Three field (travel) blanks were prepared for each batch of samples, analyzed together with those samples, and used to blank correct sample results and determine the minimum detection limits (MDL). From the field blanks, the MDL was calculated to be 0.31 μg m^{-3} for a one-week ALPHA passive NH_3 sample. All lab measurements were conducted in the Key Laboratory of Plant-Soil Interactions, Chinese Ministry of Education, China Agricultural University. More details of the passive samplers and related laboratory preparation and analysis can be found in Xu et al. (2015).

2.3 Meteorological data

Meteorological parameters, including wind speed (WS), wind direction (WD), relative humidity (RH), and temperature (T), were obtained at all sampling heights except 2 m, and the temperature was not available at 8 m. WS and WD were measured using four-cup anemometers (model O1OC, Met One Instruments), and RH and T were measured using a T/RH sensor (model HC2-S3, ROTRONIC).

2.4 Data analysis

Repeated-measures analysis of variance (ANOVA) was used to test changes in NH_3 concentration along vertical profiles. When the ANOVA results were significant, the Tukey's Honest Significant Difference (HSD) test was used to determine the significance of the difference between means with a significance level of $P < 0.05$. The coefficient of determination was used to test the linear correlations with a significance level of $P < 0.05$. All the statistical analyses were conducted using SPSS Version 23.0 (IBM Corp., Armonk, NY, USA).

Potential source contribution function analysis (PSCF) (Ashbaugh et al., 1985) of atmospheric NH_3 was performed using MeteoInfo (TrajStat package) (Wang, 2014), where 72 h back trajectories arriving at the monitoring site (IAP tower) at each height were calculated every 3 h for the entire study period. The average NH_3 concentration for each cluster was computed using the cluster statistics function. NH_3 pathways could then be associated with the high concentration clusters. The number of trajectory segment endpoints falling in a grid cell (i, j) is n_{ij}. The number of trajectory endpoints associated with the data with the concentration of NH_3 concentrations higher than an arbitrarily set criterion for each height during the

Atmos. Chem. Phys. Discuss., https://doi.org/10.5194/acp-2018-762
Manuscript under review for journal Atmos. Chem. Phys.
Discussion started: 3 September 2018

four seasons (75th percentile for NH_3 was set here) is m_{ij} (Table S1). The PSCF value for the ij th cell is then calculated as m_{ij}/n_{ij}. A weighting function W_{ij} was applied to reduce the uncertainties of small values of n_{ij} (Polissar et al., 1999). Weighted PSCF values (WPSCF) were calculated by multiplying a particular W_{ij} (≤1.00) if the total number of the endpoints for one grid cell was lower than three times the average of the endpoints per each cell. Higher WPSCF values indicate higher potential contributions of NH_3 to the receptor site (IAP tower).

$$w_{ij} = \begin{cases} 1.00 & 80 < n_{ij} \\ 0.70 & 20 < n_{ij} \leq 80 \\ 0.42 & 10 < n_{ij} \leq 20 \\ 0.05 & n_{ij} \leq 10 \end{cases}$$

3. Results

3.1 Vertical profiles of NH_3 concentrations

The time series of weekly averages of NH_3 concentrations during March 16, 2016 - March 16, 2017 are shown in Fig. 2. The weekly NH_3 concentration across all heights averaged 13.3±4.8 μg m^{-3} during the year-long study period. Individual weekly concentrations ranged from 4.4 μg m^{-3} at 2 m to 25.3 μg m^{-3} at 32 m. Nearly all (99.6%) of the weekly NH_3 concentrations along the profile exceeded 5 μg m^{-3}. Summer concentrations were generally the highest. Maximum NH_3 concentrations mostly occurred between 32 m and 63 m, decreasing both towards the surface and the top of the tower. Minimum concentrations mostly occurred at 2 m and 320 m (Fig. S1). Significant differences of annual average NH_3 concentrations across the vertical profile were only found between the "maximum concentration" height and the top two heights, i.e. 280 m and 320 m (Fig. 3i). Even at 320 m, the annual average NH_3 concentration was still relatively high at 11.3 μg m^{-3} (Fig. 3i). During the whole Beijing observation period, the daily average boundary layer height was generally above 320 m, indicating a good portion of the sampling occurred within a well-mixed boundary layer (Fig. S2).

Seasonal vertical concentration profiles exhibited shapes that were fairly similar to the annual average profile, but with some important differences in absolute concentration values and the magnitude of vertical gradients within the profiles (Fig. 3). The average NH_3 concentration across the profile from high to low was observed in summer (18.2 μg m^{-3}), spring (13.4 μg m^{-3}), autumn (12.1 μg m^{-3}), and winter (8.3 μg m^{-3}). Proportional declines of NH_3 concentration from the peak to higher and lower elevations differed between seasons, being greatest in autumn (28.3% decrease from 63 m to 320 m), and winter (27.8%) followed by summer (19.7%) and spring (15.4%) (Fig. S3).

3.2 Meteorological variability

Vertical NH_3 concentration profiles varied substantially during the sampling period, along with vertical changes in meteorological parameters. Bivariate polar plots (Fig. 4) show that high NH_3 concentrations below 47 m were mostly observed during periods with low wind speeds (< 4 m s^{-1}). As heights and associated wind speeds increased, the relationship between NH_3 concentrations and wind speed weakened. For example, at 280 m, the highest concentration was observed when the wind speed was also high (up to an average of ~15 m s^{-1}).

Wind directions play an important role in air pollution transport. Transport from the northwest was typically associated with low NH_3 concentrations at all heights, consistent with the relative lack of large emissions sources in the mountains NW of Beijing. It is noteworthy that high NH_3 concentrations at near-surface heights (8 m and 15 m) always coincide with winds from the south, including southeast and southwest directions. High NH_3 concentrations appear to be associated with winds from the northeast from 32 m until 80 m. Above 80 m, winds from the south contribute more to high NH_3 concentrations. Major regions of agricultural NH_3 emissions are located south and east of Beijing.

To further investigate observed variability, we show the probability density function of NH_3 concentrations in relation to the relative humidity (RH) and temperature (T) (Fig. 5). Clear positive relationships between T and NH_3 concentrations were found at all heights from low RH to high RH. When T was low (T<12℃), the NH_3 concentration fell mostly below 10 μg m^{-3} under any RH condition. The occurrence of high NH_3 concentrations increased with higher T>12℃, which is not surprising, given that agricultural NH_3 emissions increase with T while higher T and lower RH also shift the equilibrium of the $NH_3(g) + HNO_3(g) \leftrightarrow NH_4NO_3(p)$ system toward the gas phase. Statistically, a strong positive relationship was found between NH_3 and T at all heights from the surface to the top of the tower (R^2 ~0.6) (Fig. S4); both slope and correlation coefficients were similar across all heights. Although, a positive correlation between NH_3 and RH and a negative correlation between NH_3 and wind speed (WS) were found, the correlation coefficients were quite low.

3.3 Potential source analysis

Analysis of the relationship between local wind direction and NH_3 concentrations does not fully clarify the potential source regions contributing to observed ammonia at the sampling site (Fig. S6). Some variations were observed related to season such as NH_3 concentration increased as wind sectors changed from northwest to south in the spring, higher concentrations were associated with southerly and easterly winds in the summer and autumn, and NH_3 concentrations still exceeded 5 μg m^{-3} during winter with relatively frequent winds from north and northwest.

To examine the relationship between air transport and ammonia concentrations more rigorously, weighted PSCF (WPSCF) during the four seasons were calculated for several measurement heights (2, 63, 180, 320 m) (Fig. 6). In summer, from the surface to the tower top, strong influence is seen from source areas south of Beijing, coinciding with regions (e.g. Tianjin, Henan, Hebei and Shandong provinces) characterized by elevated anthropogenic emissions of NH_3 (Fig. 1), largely from agricultural activities (Zhang et al., 2009; Gu et al., 2012). During summer, regions to the north and west of the monitoring site had low WPSCF values. High WPSCF values to the south and southeast were common during spring. High WPSCF values were mainly located northwest and southeast of Beijing in autumn, while there WPSCF values were typically lower in winter than during other seasons.

It is important to remember that aerosol-gas partitioning can also strongly influence measured NH_3 concentrations. To investigate seasonal phase changes between NH_3 and NH_4^+, we define the ammonia gas fraction (F_{NH3} = the gaseous NH_3 concentration divided by the sum of the gaseous NH_3 and fine particulate NH_4^+ concentrations), where the concentrations are expressed in molar units. Monthly average partitioning for these reduced inorganic nitrogen forms from a nearby urban monitoring site, 10 km away from the IAP tower, is plotted in Fig. S8. The NH_3 gas fraction (F_{NH3}) was found to be high in summer (0.83 in August) and lowest in winter (0.36 in February). As expected, gas phase NH_3 is favored in the warmer months, while particle phase NH_4^+ is favored for the cooler months, with a gradual transition. Weekly NH_4^+ concentrations at the tower were estimated using weekly NH_3 concentrations divided by monthly F_{NH3}, then, WPSCF analysis of the sum of NH_3+NH_4^+ was performed (see results in Fig. S9. Results of this total WPSCF (NH_3+NH_4^+) analysis yielded similar

Atmos. Chem. Phys. Discuss., https://doi.org/10.5194/acp-2018-762
Manuscript under review for journal Atmos. Chem. Phys.
Discussion started: 3 September 2018

patterns to the NH_3 WPSCF analysis for all heights and seasons, indicating the importance of the identified source regions for both the gaseous and particulate atmospheric forms of emitted NH_3.

4. Discussion

4.1 Vertical NH_3 concentration profiles

The North China Plain is a well-known "hotspot" for NH_3 emissions due to the rapid development of industrialization, urbanization and intensive agriculture (Kang et al., 2016; Zhang et al., 2010). In our study, high atmospheric NH_3 concentrations (13.3±4.8 μg m^{-3}) were found up to 320 m above ground level in urban Beijing (March 16th, 2016 - March 16th, 2017), much higher than the average annual NH_3 concentration (3.3±1.4 μg m^{-3}) observed across a vertical profile at the 300 m USA rural BAO tower (Li et al., 2017). Some studies of NH_3 vertical distribution found that the NH_3 concentration significantly decreased with height. For example, Tevlin et al. (2017) reported an overall increase in summertime NH_3 mixing ratios toward the surface of 6.7 ppb or 5.1 μg m^{-3} (89%) during the day and 3.9 ppb or 3.0 μg m^{-3} (141%) at night. In the BAO tower study (Li et al., 2017), which also measured concentrations using passive (Radiello) samplers deployed for one to two week sample periods, the concentration profiles showed a similar overall vertical distribution. The minimum NH_3 concentration was at the top, slowly increasing towards a peak concentration at ~10 m before a sharp reduction near the surface. By contrast, our results showed much smaller decreases in NH_3 concentrations in upper air in urban Beijing (Table 1), with only a 1.18 μg m^{-3} (9.5%) average decrease from the surface to the top (Fig. 3i). The flatter shape of the Beijing vertical profile may reflect a combination of strong local (e.g. vehicle) and regional (e.g. industrial and agricultural emissions) sources (Fig. 2 and Fig.6) in our study, the fact that deep mixing layers regularly enveloped the full height of the tower within the surface boundary layer so that all sources influencing the tower measurements were vertically well mixed (Fig. S2), and/or the averaging of more distinct profiles over the week-long sample periods. Higher time resolution vertical profile measurements are needed in the future to untangle the influence of these potential factors.

Distinct seasonal variations in NH_3 concentrations were found (Fig. 2), statistically most strongly associated with temperature rather than relative humidity or wind speed (Fig. S4). High temperatures enhance NH_3 emissions from soil, applied fertilizers, and animal waste, can enhance vertical mixing, and increase volatilization of NH_3 from NH_4NO_3 particulate matter (Bari et al., 2003; Ianniello et al., 2010; Li et al., 2014; Lin et al., 2006; Meng et al., 2011; Plessow et al., 2005; Walker et al., 2004; Zbieranowski and Aherne, 2012). While high (low) mixed-layer heights in spring and summer (autumn and winter) could dilute (concentrate) NH_3 in the surface boundary layer (Fig. S3), average NH_3 concentrations across the profile were actually high in summer/spring and low in winter/autumn, consistent with the strong temperature-driven seasonal variation of NH_3 concentration and the greater NH_4NO_3 particle formation during cold periods in autumn and winter. Having simultaneous measurements of fine particle composition, with height, in future studies would be valuable for more closely evaluating the influence of changes in phase-partitioning.

Li et al. (2017) found (Fig. 3j) a vertical difference of approximately 75% from the concentration peak near the surface to the top of the BAO tower in winter, and attributed this strong vertical gradient to the occurrence of low level temperature inversions which trap emissions closer to the surface in winter. During our study in Beijing, the vertical gradient was only 28% in winter (maximum concentration found at 32 m), consistent with a deeper average boundary layer. Inversions, however, did limit vertical mixing of NH_3 during some periods in Beijing. Examination of thermal inversion layer probability at 6 a.m. and 3 p.m. (Fig. S7b and 7c) revealed that T inversions (0.22±0.26 °C) frequently occurred between 102 m and 160 m. Consequently, persistent higher NH_3 concentrations begin at a lower altitude (Fig. S7a) as also observed by Tevlin et al. (2017). Because the time resolution of our Beijing study was one sample per week, we could not catch the changes between the daytime and nighttime NH_3 vertical mixing. Compared to NH_3 monitoring in real time (Tevlin et al., 2017), weekly sampling smooths diurnal vertical distributions and makes it harder to identify the influence of local, surface sources or sinks.

Surfaces can act either as sources or sinks of NH_3, depending on surface NH_3 content, ambient NH_3 concentrations, and local meteorology and surface type (Tevlin et al., 2017; Zhang et al., 2010). The maximum NH_3 concentration occurrence at 2 m in Beijing and the concentration decrease with increased height may reflect an important surface source of NH_3, although our limited time resolution makes such conclusions tentative. The influence of evaporation of dew/precipitation may also be important. Some studies found that dew is both a significant night-time reservoir/sink and strong morning source of NH_3 (Wentworth et al., 2016; Teng et al., 2017).

4.2. Potential source analysis

Areas south of Beijing with high WPSCF values appear to be important NH_3 source regions (Fig. 6), suggesting regional transport from high agricultural NH_3 emission areas (e.g. Hebei, Henan, Shandong provinces etc.) contributed significantly to atmospheric NH_3 in the Beijing urban region. Consistently higher NH_3 concentrations were observed during periods with winds from the SE, S and SW at all heights, especially in summer (Fig. S6). Although NH_3 has a limited atmospheric lifetime with respect to dry deposition, concentrations in these agricultural NH_3 source regions can be extremely high (Shen et al., 2011) while significant ammonia can be tied up in longer-lived ammonium nitrate particles that partially dissociate to release NH_3 back to the gas phase in response to NH_3 loss by dry deposition (Ianniello et al., 2011; Kang et al., 2016; Xu et al., 2017). The WPSCF (Fig. 6) and NH_3 emissions distribution (Fig. 1 left) both suggest the importance not only of regional transport from nearby areas, but also the potential for local emission to play an important role in sustaining the high NH_3 level in Beijing, e.g. vehicular traffic (Chang et al., 2018; Pan et al., 2018a). As discussed above, stagnant meteorological conditions with low WS and T inversions allow local emissions, such as those from urban traffic, to accumulate. Additionally, the topography of the mountains to the west and north of Beijing effectively traps polluted air over Beijing during southerly airflow, an effect reported in many Beijing particulate matter studies (Xia et al., 2016; Wu et al., 2009; Zhao et al., 2009).

Generally, NH_3 source regions identified in WPSCF analysis (Fig. 6) suggested that regional transport from the south exerts an important influence on Beijing NH_3 concentrations throughout the year. The area south of Beijing (e.g Hebei, Henan and Shandong provinces) is a hotspot of NH_3 emission (Zhang et al., 2018) and half of NH_3 emissions have been estimated to deposit as NH_3 at urban sites in North China Plain (Pan et al., 2018b). In addition, seasonal patterns of NH_3 potential sources (Fig. 6) matched well with the seasonal surface NH_3 concentrations in China (Zhang et al., 2018). In detail, NH_3 concentrations were typically highest in summer and south winds produced higher NH_3 concentrations than other summer wind directions (Fig. S6). Spring and summer had a similar wind direction distribution (Fig. S6) and wind speeds (Fig. S5), but corresponding NH_3 concentrations were lower in spring. This may reflect decreased emissions in regions to the south during cooler spring temperatures and increased partitioning of NH_3 into fine particles during this cooler season. As shown above aerosol-gas partitioning strongly influences NH_3 concentrations; high F_{NH3} during warm periods, especially summer, favored greater NH_3 gas concentrations due to the thermodynamic tendency for NH_4NO_3 to dissociate to NH_3 and HNO_3 at high temperature. Although F_{NH3} was low in winter, indicating NH_4^+ is the dominant NH_x form in this cold season, winter NH_3 concentrations across all heights still averaged 8.3±2.6 μg m^{-3}, with a similar wind direction distribution as other seasons, except at high altitudes (i.e. 240 m and 320 m, Fig. S6).

5. Conclusions and implications

Our study is the first to continually monitor the vertical concentration profile of NH_3 in urban Beijing. Weekly concentrations were measured for one year at 16 heights on the 325 m Beijing meteorological tower. The NH_3 concentration averaged 13.3±4.8 μg m^{-3}. Highest NH_3 concentrations were always observed at 32-63 m height, decreasing toward the surface and toward higher altitudes.

NH_3 concentrations at all heights increased during warmer periods, consistent with increased NH_3 emissions under warm conditions and the tendency for semivolatile ammonium nitrate to release NH_3 to the gas phase. Analysis of the relationship between NH_3 concentrations and local wind direction showed a tendency for higher concentrations during transport from regions to the south of Beijing, consistent with findings from WPSCF analysis that showed that important source areas were mainly located to the south of Beijing, consistent with large agricultural regions and high NH_3 emissions in the North China Plain. Local NH_3 sources, such as urban traffic emissions, may also help account for the elevated NH_3 concentrations (> 5 μg m^{-3}) observed even in periods when transport came mostly from low NH_3 mountainous regions to Beijing's north/northwest.

High NH_3 concentrations in urban Beijing, from the surface up to 320 m, the important role that NH_3 plays in $PM_{2.5}$ and haze formation, and the importance of regional transport of NH_3 emissions from agricultural regions in neighboring provinces, suggest that future air quality improvement efforts should consider NH_3 emission reductions and that the pollution controls should be jointly practiced at regional scales (e.g. the whole North China Plain) rather than only controlling local Beijing sources.

Acknowledgements. This work was supported by the State Key Research & Development Programme (2016YFC0207906, 2017YFC0210100, DQGG0208), the National Natural Science Foundation of China (41425007), and the National Postdoctoral Program for Innovative Talents (BX201600157).

References

Ashbaugh, L. L., Malm, W. C., and Sadeh, W. Z.: A residence time probability analysis of sulfur concentrations at Grand Canyon National Park, Atmos. Environ. (1967), 19, 1263-1270, https://doi.org/10.1016/0004-6981(85)90256-2, 1985.

Bari, A., Ferraro, V., Wilson, L. R., Luttinger, D., and Husain, L.: Measurements of gaseous HONO, HNO_3, SO_2, HCl, NH_3, particulate sulfate and $PM_{2.5}$ in New York, NY, Atmos. Environ. , 37, 2825-2835, https://doi.org/10.1016/S1352-2310(03)00199-7, 2003.

Chang, Y., Liu, X., Deng, C., Dore, A. J., and Zhuang, G.: Source apportionment of atmospheric ammonia before, during, and after the 2014 APEC summit in Beijing using stable nitrogen isotope signatures, Atmos. Chem. Phys. , 16, 11635-11647, https://doi.org/10.5194/acp-16-11635-2016, 2016.

Dammers, E., Schaap, M., Haaima, M., Palm, M., Kruit, R. W., Volten, H., Hensen, A., Swart, D., and Erisman, J.: Measuring atmospheric ammonia with remote sensing campaign: Part 1–Characterisation of vertical ammonia concentration profile in the centre of The Netherlands, Atmos. Environ. , 169, 97-112, https://doi.org/10.1016/j.atmosenv.2017.08.067, 2017.

EMEP Webdab emission data hosted by the Centre on Emission Inventories and Projections (CEIP): http://www.ceip.at, access: 20 August, 2009.

Erisman, J. W., Vermetten, A. W., Asman, W. A., Waijers-Ijpelaan, A., and Slanina, J.: Vertical distribution of gases and aerosols: the behaviour of ammonia and related components in the lower atmosphere, Atmos. Environ. (1967), 22, 1153-1160, https://doi.org/10.1016/0004-6981(88)90345-9, 1988.

Erisman, J. W., Sutton, M. A., Galloway, J., Klimont, Z., and Winiwarter, W.: How a century of ammonia synthesis changed the world, Nat. Geosci. , 1, 636-639, https://doi.org/10.1038/ngeo325, 2008.

Fowler, D., Pilegaard, K., Sutton, M., Ambus, P., Raivonen, M., Duyzer, J., Simpson, D., Fagerli, H., Fuzzi, S., and Schjørring, J. K.: Atmospheric composition change: ecosystems–atmosphere interactions, Atmos. Environ. , 43, 5193-5267, https://doi.org/10.1016/j.atmosenv.2009.07.068, 2009.

Fu, X., Wang, S., Xing, J., Zhang, X., Wang, T., and Hao, J.: Increasing Ammonia Concentrations Reduce the Effectiveness of Particle Pollution Control Achieved via SO_2 and NO_x Emissions Reduction in East China, Environ. Sci. Technol. Letters, 4, 221-227, https://doi.org/10.1021/acs.estlett.7b00143, 2017.

Galloway, J. N., Aber, J. D., Erisman, J. W., Seitzinger, S. P., Howarth, R. W., Cowling, E. B., and Cosby, B. J.: The nitrogen cascade, AIBS Bulletin, 53, 341-356, https://doi.org/10.1641/0006-3568(2003)053[0341:TNC]2.0.CO;2, 2003.

Gu, B., Ge, Y., Ren, Y., Xu, B., Luo, W., Jiang, H., Gu, B., and Chang, J.: Atmospheric reactive nitrogen in China: Sources, recent trends, and damage costs, Environ. Sci. Technol. , 46, 9420-9427, https://doi.org/10.1021/es301446g, 2012.

Gu, B., Sutton, M. A., Chang, S. X., Ge, Y., and Chang, J.: Agricultural ammonia emissions contribute to China's urban air pollution, Front. Ecol. Environ., 12, 265-266, https://doi.org/10.1890/14.WB.007, 2014.

Guo, S., Hu, M., Zamora, M. L., Peng, J., Shang, D., Zheng, J., Du, Z., Wu, Z., Shao, M., and Zeng, L.: Elucidating severe urban haze formation in China, Proceedings of the National Academy of Sciences of the United States of America, 111, 17373-17378, https://doi.org/10.1073/pnas.1419604111, 2014.

Huang, R., Zhang, Y., Bozzetti, C., Ho, K., Cao, J., Han, Y., Daellenbach, K. R., Slowik, J. G., Platt, S. M., and Canonaco, F.: High secondary aerosol contribution to particulate pollution during haze events in China, Nature, 514, 218-222, https://doi.org/10.1038/nature13774, 2014.

Ianniello, A., Spataro, F., Esposito, G., Allegrini, I., Rantica, E., Ancora, M., Hu, M., and Zhu, T.: Occurrence of gas phase ammonia in the area of Beijing (China), Atmos. Chem. Phys. , 10, 9487-9503, https://doi.org/10.5194/acp-10-9487-2010, 2010.

Ianniello, A., Spataro, F., Esposito, G., Allegrini, I., Hu, M., and Zhu, T.: Chemical characteristics of inorganic ammonium salts in $PM_{2.5}$ in the atmosphere of Beijing (China), Atmos. Chem. Phys. , 11, 10803-10822, https://doi.org/10.5194/acp-11-10803-2011, 2011.

Kang, Y., Liu, M., Song, Y., Huang, X., Yao, H., Cai, X., Zhang, H., Kang, L., Liu, X., and Yan, X.: High-resolution ammonia emissions inventories in China from 1980 to 2012, Atmos. Chem. Phys. , 16, 2043-2058, https://doi.org/10.5194/acp-16-2043-2016, 2016.

Klimont, Z.: Current and Future Emissions of Ammonia in China, 10th annual emission inventory conference: one atmosphere, One inventory, many challenges, 1-3, May, 2001

LeBel, P. J., Hoell, J. M., Levine, J. S., and Vay, S. A.: Aircraft measurements of ammonia and nitric acid in the lower troposphere, Geophys. Res. Lett. , 12, 401-404, https://doi.org/10.1029/GL012i006p00401, 1985.

Lee, D., Dollard, G., Derwent, R., and Pepler, S.: Observations on gaseous and aerosols components of the atmosphere and their relationships, Water, Air, and Soil Pollution, 113, 175-202, 1999.

Li, P., Yan, R., Yu, S., Wang, S., Liu, W., and Bao, H.: Reinstate regional transport of $PM_{2.5}$ as a major cause of severe haze in Beijing, Proceedings of the National Academy of Sciences of the United States of America, 112, E2739-E2740, https://doi.org/10.1073/pnas.1502596112, 2015.

Li, Y., Schwandner, F. M., Sewell, H. J., Zivkovich, A., Tigges, M., Raja, S., Holcomb, S., Molenar, J. V., Sherman, L., and Archuleta, C.: Observations of ammonia, nitric acid, and fine particles in a rural gas production region, Atmos. Environ. , 83, 80-89, https://doi.org/10.1016/j.atmosenv.2013.10.007, 2014.

Li, Y., Thompson, T. M., Damme, M. V., Chen, X., Benedict, K. B., Shao, Y., Day, D., Boris, A., Sullivan, A. P., and Ham, J.: Temporal and spatial variability of ammonia in urban and agricultural regions of northern Colorado, United States, Atmos. Chem. Phys. , 17, 6197-6213, https://doi.org/10.5194/acp-17-6197-2017, 2017.

Lin, Y., Cheng, M., Ting, W., and Yeh, C.: Characteristics of gaseous HNO_2, HNO_3, NH_3 and particulate ammonium nitrate in an urban city of Central Taiwan, Atmos. Environ. , 40, 4725-4733, https://doi.org/10.1016/j.atmosenv.2006.04.037, 2006.

Meng, Z., Lin, W., Jiang, X., Yan, P., Wang, Y., Zhang, Y., Jia, X., and Yu, X.: Characteristics of atmospheric ammonia over Beijing, China, Atmos. Chem. Phys. , 11, 6139-6151, https://doi.org/10.5194/acp-11-6139-2011, 2011.

Öztürk, F., Bahreini, R., Wagner, N., Dubé, W., Young, C., Brown, S., Brock, C., Ulbrich, I., Jimenez, J., and Cooper, O.: Vertically resolved chemical characteristics and sources of submicron aerosols measured on a Tall Tower in a suburban area near Denver, Colorado in winter, J. Geophys. Res. [Atmos.], 118, 13591-13605, https://doi.org/10.1002/2013JD019923, 2013.

Pan, Y., Tian, S., Liu, D., Fang, Y., Zhu, X., Gao, M., Gao, J., Michalski, G., and Wang, Y.: Isotopic evidence for enhanced fossil fuel sources of aerosol ammonium in the urban atmosphere, Environ. Pollut. , 238, 942-947, https://doi.org/10.1016/j.envpol.2018.03.038, 2018a.

Pan, Y., Tian, S., Zhao, Y., Zhang, L., Zhu, X., Gao, J., Huang, W., Zhou, Y., Song, Y., and Zhang, Q.: Identifying ammonia hotspots in China using a national observation network, Environ. Sci. Technol. , 52, 3926-3934, https://doi.org/10.1021/acs.est.7b05235, 2018b.

Plessow, K., Spindler, G., Zimmermann, F., and Matschullat, J.: Seasonal variations and interactions of N-containing gases and particles over a coniferous forest, Saxony, Germany, Atmos. Environ. , 39, 6995-7007, https://doi.org/10.1016/j.atmosenv.2005.07.046, 2005.

Polissar, A., Hopke, P., Paatero, P., Kaufmann, Y., Hall, D., Bodhaine, B., Dutton, E., and Harris, J.: The aerosol at Barrow, Alaska: long-term trends and source locations, Atmos. Environ. , 33, 2441-2458, https://doi.org/10.1016/S1352-2310(98)00423-3, 1999.

Quan, J., Gao, Y., Zhang, Q., Tie, X., Cao, J., Han, S., Meng, J., Chen, P., and Zhao, D.: Evolution of planetary boundary layer under different weather conditions, and its impact on aerosol concentrations, Particuology, 11, 34-40, https://doi.org/10.1016/j.partic.2012.04.005, 2013.

Reis, S., Pinder, R., Zhang, M., Lijie, G., and Sutton, M.: Reactive nitrogen in atmospheric emission inventories, Atmos. Chem. Phys. , 9, 7657-7677, https://doi.org/10.5194/acp-9-7657-2009, 2009.

Riedel, T. P., Wagner, N. L., Dubé, W. P., Middlebrook, A. M., Young, C. J., Öztürk, F., Bahreini, R., VandenBoer, T. C., Wolfe, D. E., and Williams, E. J.: Chlorine activation within urban or power plant plumes: Vertically resolved $ClNO_2$ and Cl_2 measurements from a tall tower in a polluted continental setting, J. Geophys. Res. [Atmos.], 118, 8702-8715, https://doi.org/10.1002/jgrd.50637, 2013.

Shen, J., Liu, X., Zhang, Y., Fangmeier, A., Goulding, K., and Zhang, F.: Atmospheric ammonia and particulate ammonium from agricultural sources in the North China Plain, Atmos. Environ. , 45, 5033-5041, https://doi.org/10.1016/j.atmosenv.2011.02.031, 2011.

Shephard, M., and Cady-Pereira, K.: Cross-track Infrared Sounder (CrIS) satellite observations of tropospheric ammonia, Atmos. Meas. Tech., 8, 1323-1336, https://doi.org/10.5194/amt-8-1323-2015, 2015.

Sun, K., Tao, L., Miller, D. J., Zondlo, M. A., Shonkwiler, K. B., Nash, C., and Ham, J. M.: Open-path eddy covariance measurements of ammonia fluxes from a beef cattle feedlot, Agric. For. Meteorol. , 213, 193-202, https://doi.org/10.1016/j.agrformet.2015.06.007, 2015.

Sun, K., Tao, L., Miller, D. J., Pan, D., Golston, L. M., Zondlo, M. A., Griffin, R. J., Wallace, H. W., Leong, Y. J., and Yang, M. M.: Vehicle emissions as an important urban ammonia source in the United States and China, Environ. Sci. Technol. , 51, 2472-2481, https://doi.org/10.1021/acs.est.6b02805, 2017.

Sun, Y., Jiang, Q., Wang, Z., Fu, P., Li, J., Yang, T., and Yin, Y.: Investigation of the sources and evolution processes of severe haze pollution in Beijing in January 2013, J. Geophys. Res. [Atmos.], 119, 4380-4398, https://doi.org/10.1002/2014JD021641, 2014.

Sun, Y., Du, W., Fu, P., Wang, Q., Li, J., Ge, X., Zhang, Q., Zhu, C., Ren, L., and Xu, W.: Primary and secondary aerosols in Beijing in winter: sources, variations and processes, Atmos. Chem. Phys. , 16, 8309-8329, https://doi.org/10.5194/acp-16-8309-2016, 2016.

Sutton, M. A., Erisman, J. W., Dentener, F., and Möller, D.: Ammonia in the environment: from ancient times to the present, Environ. Pollut. , 156, 583-604, https://doi.org/10.1016/j.envpol.2008.03.013, 2008.

Tang, G., Zhu, X., Hu, B., Xin, J., Wang, L., Münkel, C., Mao, G., and Wang, Y.: Impact of emission controls on air quality in Beijing during APEC 2014: lidar ceilometer observations, Atmos. Chem. Phys. , 15, 12667-12680, https://doi.org/10.5194/acp-15-12667-2015, 2015.

Teng, X., Hu, Q., Zhang, L., Qi, J., Shi, J., Xie, H., Gao, H., and Yao, X.: Identification of major sources of atmospheric NH_3 in an urban environment in northern China during wintertime, Environ. Sci. Technol. , 51, 6839-6848, https://doi.org/10.1021/acs.est.7b00328, 2017.

Tevlin, A., Li, Y., Collett, J., McDuffie, E., Fischer, E., and Murphy, J.: Tall tower vertical profiles and diurnal trends of ammonia in the Colorado Front Range, J. Geophys. Res. [Atmos.], 122, 12468-12487, https://doi.org/10.1002/2017JD026534, 2017.

USEPA National Emission Inventory Tier Summaries: https://www.epa.gov/ttn/chief/eiinformation.html, access: 14 August 2009.

Van Damme, M., Clarisse, L., Dammers, E., Liu, X., Nowak, J., Clerbaux, C., Flechard, C., Galy-Lacaux, C., Xu, W., and Neuman, J.: Towards validation of ammonia (NH_3) measurements from the IASI satellite, Atmos. Meas. Tech., 8, 1575-1591, https://doi.org/10.5194/amt-8-1575-2015. 2015.

VandenBoer, T. C., Brown, S. S., Murphy, J. G., Keene, W. C., Young, C. J., Pszenny, A., Kim, S., Warneke, C., Gouw, J. A., and Maben, J. R.: Understanding the role of the ground surface in HONO vertical structure: High resolution vertical profiles during NACHTT-11, J. Geophys. Res. [Atmos.], 118, 10155-10171, https://doi.org/10.1002/jgrd.50721, 2013.

Vogt, E., Held, A., and Klemm, O.: Sources and concentrations of gaseous and particulate reduced nitrogen in the city of Münster (Germany), Atmos. Environ. , 39, 7393-7402, https://doi.org/10.1016/j.atmosenv.2005.09.012, 2005.

Walker, J., Whitall, D. R., Robarge, W., and Paerl, H. W.: Ambient ammonia and ammonium aerosol across a region of variable ammonia emission density, Atmos. Environ. , 38, 1235-1246, https://doi.org/10.1016/j.atmosenv.2003.11.027, 2004.

Wang, S., Xing, J., Jang, C., Zhu, Y., Fu, J. S., and Hao, J.: Impact assessment of ammonia emissions on inorganic aerosols in East China using response surface modeling technique, Environ. Sci. Technol. , 45, 9293-9300, https://doi.org/10.1021/es2022347, 2011.

Wang, S., Nan, J., Shi, C., Fu, Q., Gao, S., Wang, D., Cui, H., Saiz-Lopez, A., and Zhou, B.: Atmospheric ammonia and its impacts on regional air quality over the megacity of Shanghai, China, Sci. Rep., 5, 15842, https://doi.org/10.1038/srep15842, 2015.

Wang, Y.: MeteoInfo: GIS software for meteorological data visualization and analysis, Meteorological Applications, 21, 360-368, https://doi.org/10.1002/met.1345, 2014.

Wentworth, G. R., Murphy, J. G., Benedict, K. B., Bangs, E. J., and Collett Jr, J. L.: The role of dew as a night-time reservoir and morning source for atmospheric ammonia, Atmos. Chem. Phys. , 16, 7435-7449, https://doi.org/10.5194/acp-16-7435-2016, 2016.

Wiegner, M., Emeis, S., Freudenthaler, V., Heese, B., Junkermann, W., Münkel, C., Schäfer, K., Seefeldner, M., and Vogt, S.: Mixing layer height over Munich, Germany: Variability and comparisons of different methodologies, J. Geophys. Res. [Atmos.], 111, D13201, https://doi.org/10.1029/2005JD006593, 2006.

Wu, Y., Gu, B., Erisman, J. W., Reis, S., Fang, Y., Lu, X., and Zhang, X. $PM_{2.5}$ pollution is substantially affected by ammonia emissions in China, Environ. Pollut., 218, 86-94, https://doi.org/10.1016/j.envpol.2016.08.027, 2016

Wu, Z., Hu, M., Shao, K., and Slanina, J.: Acidic gases, NH_3 and secondary inorganic ions in PM10 during summertime in Beijing, China and their relation to air mass history, Chemosphere, 76, 1028-1035, https://doi.org/10.1016/j.chemosphere.2009.04.066, 2009.

Xia, Y., Zhao, Y., and Nielsen, C. P.: Benefits of China's efforts in gaseous pollutant control indicated by the bottom-up emissions and satellite observations 2000–2014, Atmos. Environ. , 136, 43-53, https://doi.org/10.1016/j.atmosenv.2016.04.013, 2016.

Xu, W., Luo, X., Pan, Y. , Zhang, L., Tang, A., Shen, J., Zhang, Y., Li, K., Wu, Q., Yang, D., Zhang, Y., Xue, J., Li, W., Li, Q., Tang, L., Lu, S., Liang, T., Tong, Y., Liu, P., Zhang, Q., Xiong, Z., Shi, X., Wu, L., Shi, W., Tian, K., Zhong, X., Shi, K., Tang, Q., Zhang, L., Huang, J., He, C., Kuang, F., Zhu, B., Liu, H., Jin, X., Xin, Y., Shi, X., Du, E., Dore, A. J., Tang, S., Collett Jr., J. L., Goulding, K., Sun, Y., Ren, J., Zhang, F., and Liu, X.: Quantifying atmospheric nitrogen deposition through a nationwide monitoring network across China, Atmos. Chem. Phys. , 15, 12345-12360, https://doi.org/10.5194/acp-15-12345-2015, 2015.

Xu, W., Song, W., Zhang, Y., Liu, X., Zhang, L., Zhao, Y., Liu, D., Tang, A., Yang, D., Wang, D., Wen, Z., Pan, Y., Fowler, D., Collett Jr., J. L., Erisman, J. W., Goulding, K., Li, Y., and Zhang, F.: Air quality improvement in a megacity: implications from 2015 Beijing Parade Blue pollution control actions, Atmos. Chem. Phys. , 17, 31-46, https://doi.org/10.5194/acp-17-31-2017, 2017.

Yamamoto, N., Kabeya, N., Onodera, M., Takahahi, S., Komori, Y., Nakazuka, E., and Shirai, T.: Seasonal variation of atmospheric ammonia and particulate ammonium concentrations in the urban atmosphere of Yokohama over a 5-year period, Atmos. Environ. (1967), 22, 2621-2623, https://doi.org/10.1016/0004-6981(88)90498-2, 1988.

Yamamoto, N., Nishiura, H., Honjo, T., Ishikawa, Y., and Suzuki, K.: A long-term study of atmospheric ammonia and particulate ammonium concentrations in Yokohama, Japan, Atmos. Environ. , 29, 97-103, https://doi.org/10.1016/1352-2310(94)00226-B, 1995.

Yang, F., Tan, J., Zhao, Q., Du, Z., He, K., Ma, Y., Duan, F., Chen, G., and Zhao, Q.: Characteristics of $PM_{2.5}$ speciation in representative megacities and across China, Atmos. Chem. Phys. , 11, 5207-5219, https://doi.org/10.5194/acp-11-5207-2011, 2011.

Ye, X., Ma, Z., Zhang, J., Du, H., Chen, J., Chen, H., Yang, X., Gao, W., and Geng, F.: Important role of ammonia on haze formation in Shanghai, Environ. Res. Lett. , 6, 024019, https://doi.org/10.1088/1748-9326/6/2/024019, 2011.

Zbieranowski, A. L., and Aherne, J.: Spatial and temporal concentration of ambient atmospheric ammonia in southern Ontario, Canada, Atmos. Environ. , 62, 441-450, https://doi.org/10.1016/j.atmosenv.2012.08.041, 2012.

Zhang, L., Wright, L., and Asman, W.: Bi-directional air-surface exchange of atmospheric ammonia: A review of measurements and a development of a big-leaf model for applications in regional-scale air-quality models, J. Geophys. Res. [Atmos.], 115, D20310, https://doi.org/10.1029/2009JD013589, 2010.

Zhang, L., Chen, Y., Zhao, Y., Henze, D. K., Zhu, L., Song, Y., Paulot, F., Liu, X., Pan, Y., and Lin, Y.: Agricultural ammonia emissions in China: reconciling bottom-up and top-down estimates, Atmos. Chem. Phys. , 18, 339-355, https://doi.org/10.5194/acp-18-339-2018, 2018.

Zhang, Q., Streets, D. G., Carmichael, G. R., He, K., Huo, H., Kannari, A., Klimont, Z., Park, I. S., Reddy, S., Fu, J., Chen, D., Duan, L., Lei, Y., Wang, L., and Yao, Z.: Asian emissions in 2006 for the NASA INTEX-B mission, Atmos. Chem. Phys. , 9, 5131-5153, https://doi.org/10.5194/acp-9-5131-2009, 2009.

Zhang, X., Wu, Y., Liu, X., Reis, S., Jin, J., Dragosits, U., Damme, M. V., Clarisse, L., Whitburn, S., Coheur, P. F., and Gu, B.: Ammonia emissions may be substantially underestimated in China, Environ. Sci. Technol., 51, 12089-12096, https://doi.org/10.1021/acs.est.7b02171, 2017.

Zhang, Y., Dore, A. J., Ma, L., Liu, X., Ma, W., Cape, J.N., and Zhang, F.: Agricultural ammonia emissions inventory and spatial distribution in the North China Plain. Environ. Pollut. , 158: 490-501, https://doi.org/10.1016/j.envpol.2009.08.033, 2010.

Zhao, D., and Wang, A.: Estimation of anthropogenic ammonia emissions in Asia, Atmos. Environ. , 28, 689-694, https://doi.org/10.1016/1352-2310(94)90045-0, 1994.

Zhao, X., Zhang, X., Xu, X., Xu, J., Meng, W., and Pu, W.: Seasonal and diurnal variations of ambient $PM_{2.5}$ concentration in urban and rural environments in Beijing, Atmos. Environ. , 43, 2893-2900, https://doi.org/10.1016/j.atmosenv.2009.03.009, 2009.

Zheng, G., Duan, F., Su, H., Ma, Y., Cheng, Y., Zheng, B., Zhang, Q., Huang, T., Kimoto, T., Chang, D., Pöschl, U., Cheng, Y., and He, K.: Exploring the severe winter haze in Beijing: the impact of synoptic weather, regional transport and heterogeneous reactions, Atmos. Chem. Phys. , 15, 2969-2983, https://doi.org/10.5194/acp-15-2969-2015, 2015.

Zhou, Y., Zhu, X., Pan, Y., Tian, S., Liu, Q., Sun, Y., An, J., and Wang, Y.: Vertical distribution of gaseous pollutants in the lower atmospheric boundary layer in urban Beijing, Environmental Chemistry (in Chinese), 36, 1752-1759, 2017.

Table 1 Overview of measured vertical NH_3 concentration (μg m^{-3}) in previous studies and this study.

Heights (m) / NH_3 (μg m^{-3})	Netherlands		US BAO tower	Beijing IAS tower
	Rural area	Meteorological tower		
0~5	6.8 (1m) 6.5 (4m)	8.3	4.7	12.5
5~10	-	-	5.0	13.4
10~20	9.6	-	-	13.8
20~40	-	6.2	4.61	14.2
40~60	-	-	4.19	14.1
60~80	-	-	-	14.2
80~100	-	3.6	3.6	13.9
100~150	-	-	3.09	14.0 (120m) 13.8 (140m)
150~200	4.5	2.1	2.72	13.5 (160m) 13.3 (180m) 12.7 (200m)
200~250	-	-	2.39	12.1
250~300	-	-	2.25	11.8
300~350	-	-	-	11.3
Period	2014		12/13/2011–1/9/2013	3/16/2016–3/16/2017
References	Dammers et al. (2017)	Erisman et al. (1988)	Li et al. (2017)	This study

Atmos. Chem. Phys. Discuss., https://doi.org/10.5194/acp-2018-762
Manuscript under review for journal Atmos. Chem. Phys.
Discussion started: 3 September 2018

Atmospheric Chemistry and Physics
Open Access
Discussions

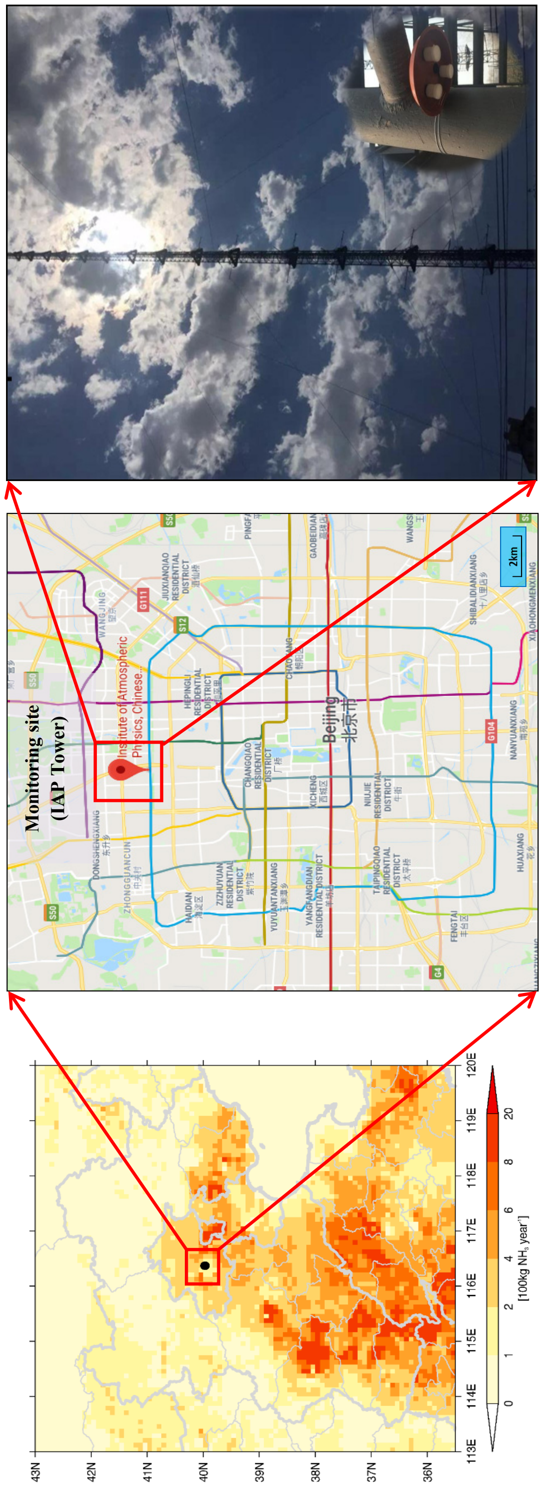

Fig. 1 Left: Modeled NH_3 emissions distribution (0.1°, ~10 km) over North China Plain in 2015 with the location of the monitoring site shown as a black dot. NH_3 emission estimates are from the inventory of Zhang et al. (2018) at 0.1° horizontal resolution. Right: Map of Beijing showing the location of the monitoring tower.

Atmos. Chem. Phys. Discuss., https://doi.org/10.5194/acp-2018-762
Manuscript under review for journal Atmos. Chem. Phys.
Discussion started: 3 September 2018

Atmospheric Chemistry and Physics Discussions
Open Access

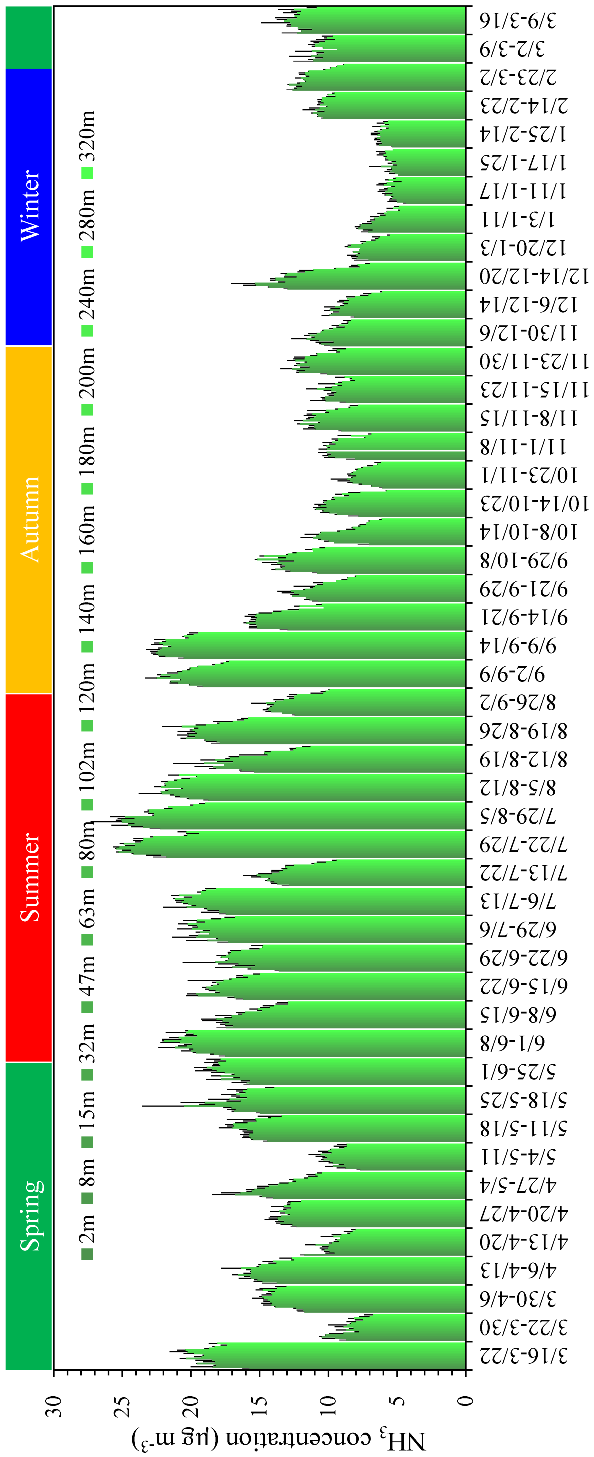

Fig. 2 Time series of vertical distribution of weekly atmospheric NH_3 concentrations (+σ) in Beijing urban (03/16/2016 - 03/16/2017)

Atmospheric Chemistry and Physics
Open Access
Discussions

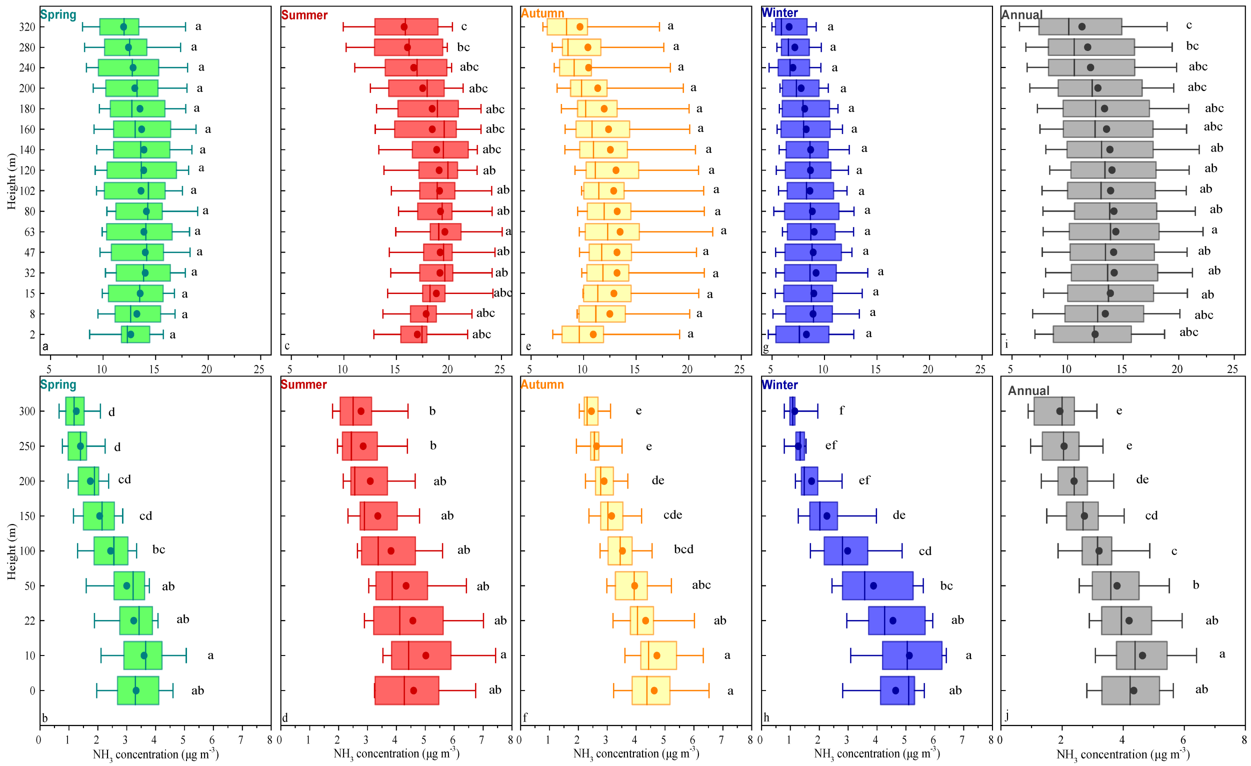

Fig. 3 Comparison of seasonal vertical NH_3 concentrations with the mean (dots), median, 10th, 25th, 75th and 90th percentiles of the NH_3 concentrations of each height for IAP tower (Beijing, this study) (fig. a, c, e, g, i) and BAO tower (USA, Li et al.,2017) (fig. b, d, f, h, j).

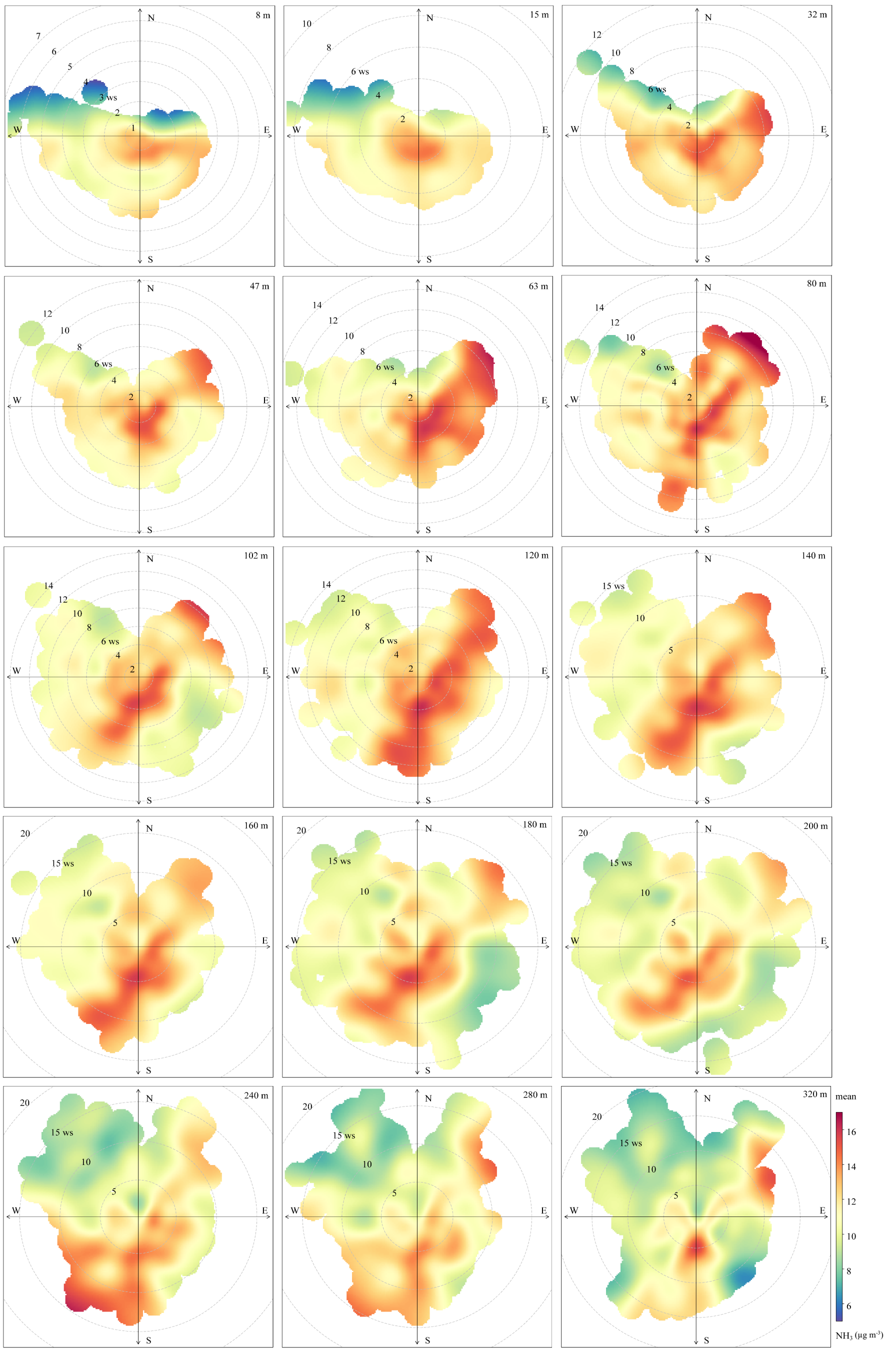

Fig. 4 The frequency distributions of wind directions and NH_3 concentration (color demarcation) for all height during the observation period. Radial data are WS (m s^{-1}) as a function of WD (°), The colors denote the NH_3 concentrations (μg m^{-3}).

Atmos. Chem. Phys. Discuss., https://doi.org/10.5194/acp-2018-762
Manuscript under review for journal Atmos. Chem. Phys.
Discussion started: 3 September 2018

Atmospheric Chemistry and Physics
Open Access
Discussions

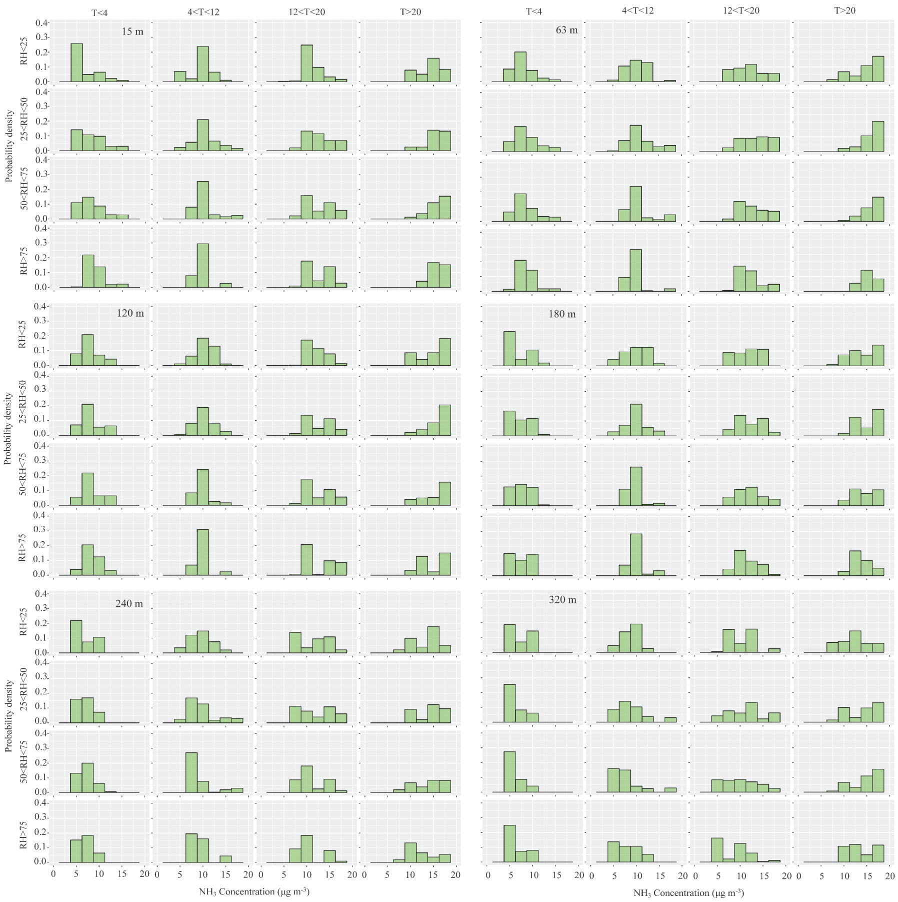

Fig. 5 Probability density of NH_3 concentration (μg m^{-3}) at different ranges of temperature* (°C) and relative humidity* (%) for 14 heights.

*** Temperature includes four subsets: <4°C, 4~12°C, 12~20°C and >20°C;**

*** Relative humidity includes four subsets: <25%, 25~50%, 50~75% and >75%.**

Atmos. Chem. Phys. Discuss., https://doi.org/10.5194/acp-2018-762
Manuscript under review for journal Atmos. Chem. Phys.
Discussion started: 3 September 2018

Atmospheric Chemistry and Physics
Open Access
Discussions

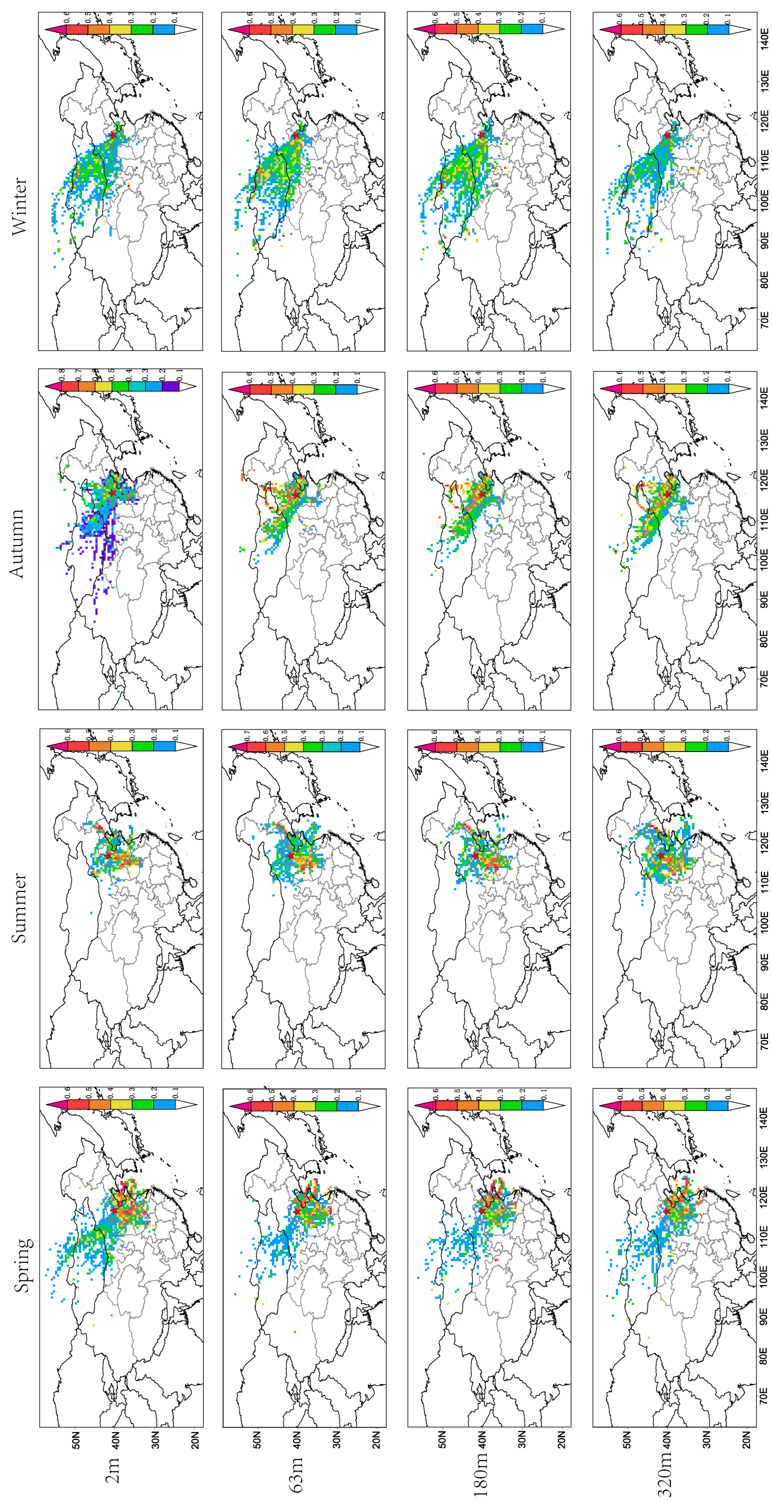

Fig. 6 Weighted potential source contribution analysis (WPSCF) of atmospheric NH_3 in Beijing during 03/16/2016 – 03/16/2017.